

Gas pressure sintering of SiC–AlN composites in nitrogen atmosphere

S. Mandal, K.K. Dhargupta, S. Ghatak*

Central Glass and Ceramic Research Institute, Non-Oxide Ceramic Section, 196 Raja SC Mullich Road, Calcutta 700 032, India

Received 26 April 2000; received in revised form 24 February 2001; accepted 5 July 2001

Abstract

The gas pressure sintering behaviour of SiC–5–25 wt.% AlN composites was studied. Sintering temperature was varied from 1700–1950 °C under a nitrogen pressure of six bar at the final sintering temperature. Pore-free dense product was achieved for the sample of composition SiC–25 wt.% AlN sintered at 1950 °C. XRD patterns revealed a gradual transformation of cubic SiC to hexagonal form with increasing sintering temperature from 1700 to 1950 °C along with the densification of the specimen and solid solution hardening. Hardness of the sample sintered at 1950 °C was found to increase with increasing AlN content from 21.26 to 25.36 GPa. © 2002 Elsevier Science Ltd and Techna S.r.l. All rights reserved.

Keywords: Gas pressure sintering; SiC–AlN composites; Nitrogen atmosphere

1. Introduction

Silicon carbide and aluminium nitride form a series of solid solutions in a very wide range [1–9,11,12] of composition. SiC–AlN solid solutions could be sintered, preferably by hot pressing in the temperature range of 1700–2300 °C [1–5,8–10,12] in inert [1–3,8,9] or nitrogen [6,7,10,12] atmosphere or in vacuum [4,5]. Pressureless sintering of such materials with liquid-phase forming additives was difficult due to the large amount of evaporation loss associated with various chemical reactions [13–15]. Densification in such systems was frequently explained by assuming liquid phase formation at the sintering temperature [6,7,10,11] during hot pressing. It is fairly established that AlN goes into solid solution in α -SiC in large proportion [5]. No positive evidence could be provided for more than 1–2% AlN solubility [4] in cubic β -SiC. But there are indications [4,5] of reactions between AlN and β -SiC transforming the later to the 2H structure. The extent of this transformation depends on the amount of AlN, and temperature and time of heat treatment of the specimen. Various structural changes that occurred during thermal processing

of those materials may thus be utilised to activate bulk diffusion by altering or suppressing decomposition reactions. Polytypic transformation temperatures of pure β -SiC were estimated to be 1600, 1800 and 2000 °C for $\beta \rightarrow 2H$, $2H \rightarrow 4H$ and $4H \rightarrow 6H$ respectively [5]. SiC–AlN phase diagram [5] also indicated a metastable β -SiC in the 1600–1800 °C temperature range. This phase was designated as β' -SiC having a large proportion of hexagonal type sites which were claimed to be responsible for AlN solubility in SiC [16–18].

Earlier workers [19,20] confirmed the existence of SiC–AlN solid solution as well as two-phase particulate composites. In SiC–AlN particulate composites SiC was present as the cubic 3C phase and AlN was present as the hexagonal 2H-phase [20]. Phase analysis by XRD revealed that the solid solutions were single-phase hexagonal 2H above 30% AlN, and the lattice parameters closely followed Vegard's law as a function of composition [21]. Though the solid solution resulted from interdiffusion between the two components, at lower sintering temperature only slight interdiffusion was observed for the two-phase composite.

In the present system sintering was performed without any additive and instead of using a free flow gas system, a gas pressure environment was maintained with varying SiC:AlN weight ratio for sintering of SiC–AlN composites. Interpretation of the results was based on

* Corresponding author. Tel.: +91-33-473-3476; fax: +91-33-473-0957.

Table 1(a)
Chemical and physical characteristics of β -SiC^a

SiC (wt.%)	Oxygen (wt.%)	Nitrogen (wt.%)	Silicon (wt.%)	Free carbon (wt.%)
98–99	0.65–0.85	0.15–0.25	0.1 (max.)	0.5–1.00

Source: superior graphite, USA.

^a size <5 μm present: 99%. Surface area, m^2/g (BET): 15+.

Table 1(b)
Chemical characteristics of AlN Source

SiC (wt.%)	Oxygen (wt.%)	Nitrogen (wt.%)	Silicon (wt.%)	Free carbon (wt.%)
Al (wt.%)	Nitrogen (wt.%)	Oxygen (wt.%)	Carbon (wt.%)	Fe (wt.%)
65.0	33.5	1.1	0.04	0.019

Source: H. C. Starck, Germany

mainly X-ray diffraction analysis of the phases formed during sintering.

2. Experimental¹

β -SiC powder and AlN powder were selected for the study of SiC–AlN composites.

2.1. Chemical composition of the raw materials

β -SiC and AlN were used as the raw materials for the present study. Specifications of the raw materials are given in the Table 1(a) and (b).

2.2. Preparation of green compacts and sintering

β -SiC powder and 5–25 wt.% of AlN powder were mixed thoroughly in acetone medium in an attritor using alumina ball. The attrited powder was wet-sieved, dried and pressed isostatically to form pellets of 20 mm diameter under a pressure of 250 MPa. The pressed pellets were sintered at 1700, 1800, 1900 and 1950 °C in a graphite resistance furnace (Astro, 1000-3560-F8204025, USA). The temperature of the furnace was sensed by a graphite/boron-graphite thermocouple. The accuracy of the measurement was ± 5 °C. The samples were put into a graphite crucible using a packing material having the same composition as that of the specimens to be sintered. A high purity N_2 gas atmosphere was maintained during sintering. The gas pressure was maintained at 6 bar at the final sintering temperature.

The heating schedule of sintering was: room temperature to 1000 °C at 15 °C/min, and 1000 °C to sintering temperature at 20 °C/min with a hold at the sintering temperature for 1 h and then the furnace power was shut-off immediately after the holding period was over.

2.3. Measurement of properties

The weight loss and shrinkage were measured for the sintered samples. Apparent porosity and bulk density were determined by Archimedes' principle. The pellets were cut cross-sectionally by a slow speed cutting machine for X-ray diffraction studies using $\text{CuK}\alpha$ target and Ni filter under 40 kV, 20 mA, on the interior surface after ultrasonic cleaning of the surface in acetone medium. Hardness values were determined by using a load of 5 N in a microhardness tester fitted with a Vicker's square pyramidal indenter.

3. Results

3.1. Weight loss

Significant weight loss was recorded for all the specimens, when sintered at 1700, 1800, 1900 and 1950 °C (Fig. 1). Increase in the amount of weight loss from 1700 to 1800 °C was not much. From 1800 to 1900 °C, a sharp increase in weight loss was recorded. Loss of weight of the specimen at 1900 and 1950 °C was almost the same with marginal increase. Therefore, it may be said that the physico-chemical phenomena responsible for weight loss were most active between 1800 to 1950 °C.

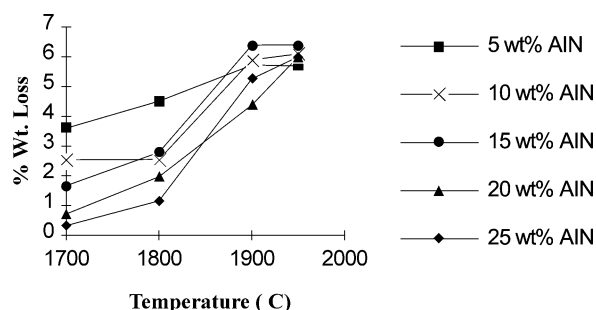


Fig. 1. Plot of wt.% loss vs. sintering temperature.

¹ Preparation part is patented in India.

Weight loss was found to be related to the amount of AlN in the composite (Fig. 2) and it decreased with increasing amount of AlN in the specimen when sintered at 1700 and 1800 °C. But, when sintering temperature was raised to 1900 and 1950 °C, weight loss of the specimen was almost independent of AlN content.

3.2. Linear shrinkage

Linear shrinkage of the specimen was small when sintered at 1700, 1800 and 1900 °C (Fig. 3). Increase in shrinkage with increase in temperature up to 1900 °C was also small. Shrinkage abruptly increased to 12.4–15.2% when the specimen was sintered at 1950 °C. This led to the elimination of pore to a large extent and a pore-free sintered product was produced with SiC–25 wt.% AlN. Thus, it may be said that complete sintering of the composites was possible only at 1950 °C. With reference to the Section 3.1 it may also be noted that increase in weight loss in the specimen and densification of the specimen took place in two stages in the temperature range 1800–1900 °C and 1900–1950 °C, respectively.

Unlike weight loss phenomenon (Fig. 2), linear shrinkage of the specimen depended much less on the amount of AlN in the composites (Fig. 4). For the specimen sintered at 1950 °C, dependence of linear shrinkage on the amount of AlN was not that significant except for SiC–25 wt.% AlN.

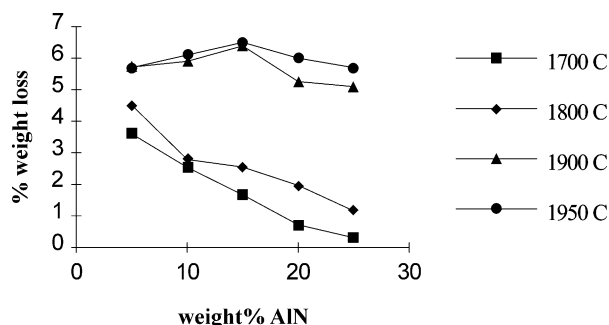


Fig. 2. Plot of wt.% loss vs. AlN content.

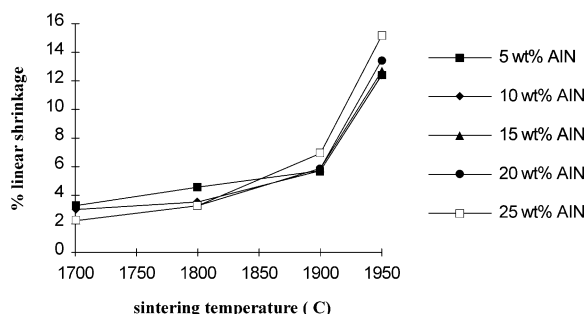


Fig. 3. Plot of linear% shrinkage vs. sintering temperature.

3.3. Bulk density

Bulk density of the specimen increased slowly up to 1900 °C (Fig. 5) and it increased abruptly when sintered at 1950 °C. Higher bulk density was always obtained with higher amount of AlN in the specimen. It may be noted that density of SiC and AlN is almost the same ($\rho_{\text{SiC}} = 3.21 \text{ g/cc}$, $\rho_{\text{AlN}} = 3.26 \text{ g/cc}$) and a mere admixture of the two compounds would not alter the density of the composites. With reference to the Sections 3.1 and 3.2 it may be said that the chemical changes in the specimen occurred, prior to the densification, in the temperature range 1800–1900 °C and the resultant reaction products may contribute towards densification at the later stage.

3.4. XRD analysis

The peak for 2H_{SS} was observed along with the peak at the d -value of 2.4883 with the relative intensity of 100.0 for the sample containing 25 wt.% AlN and the relative intensity of the peak for 2H_{SS} increased with increase in sintering temperature [Fig. 6(a)–(d)]. The peak for 6 H polytype of SiC was also observed for the sample sintered at lower temperature [Fig. 6(a) and (b)].

3.5. Hardness

Vicker's microhardness of the samples sintered at 1950 °C was found to increase from 21.26 to 25.36 GPa under a load of 5 N with increasing AlN content from 5 to 25 wt.% as shown in Fig. 7.

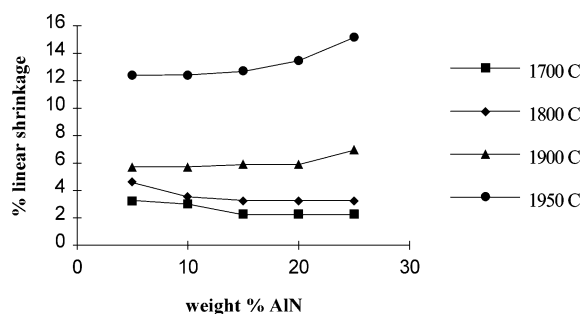


Fig. 4. Plot of linear% shrinkage vs. AlN content.

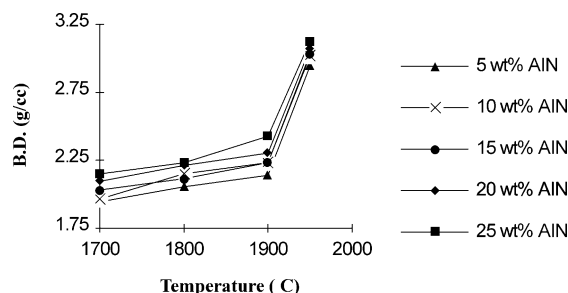


Fig. 5. Plot of B.D. (g/cc) vs. temperature of sintering.

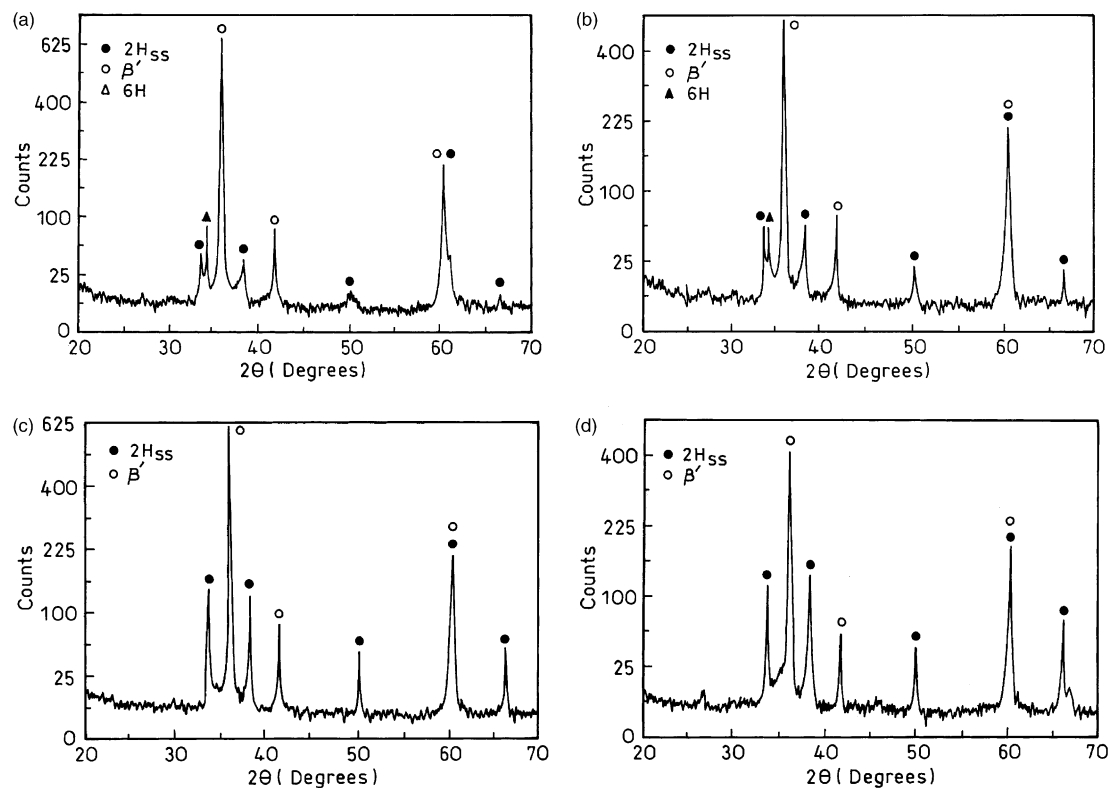


Fig. 6. XRD patterns of samples sintered with 25 wt.% AlN at (a) 1700 °C; (b) 1800 °C; (c) 1900 °C; (d) 1950 °C.

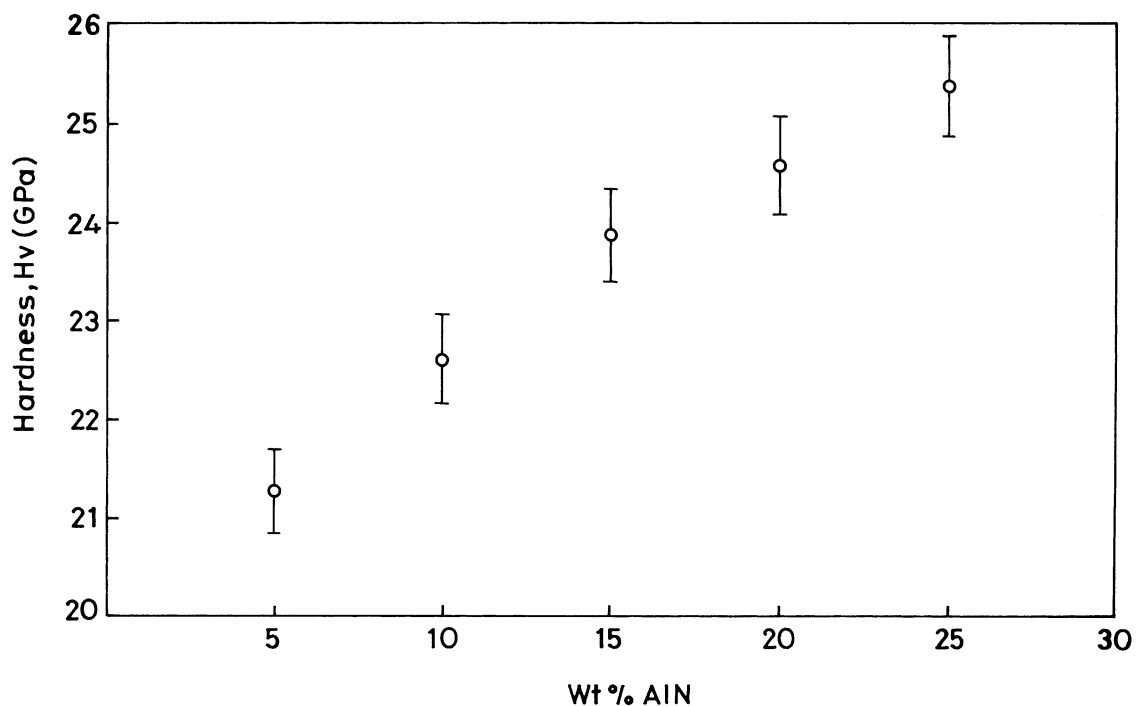
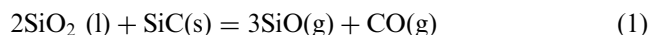


Fig. 7. Plot of Vickers microhardness (GPa) of the sample fired at 1950 °C vs. wt.% of AlN.

4. Discussion

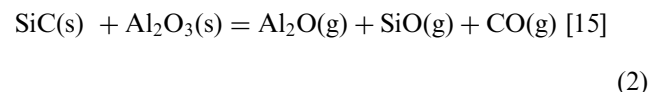
4.1. Weight changes during heat treatment

In the present system no external sintering aids [13–15] such as Y_2O_3 and Al_2O_3 were used and the components that may be identified to cause chemical reactions resulting into weight loss were SiO_2 , present as oxidation product of SiC, dissolved oxygen in AlN and SiC, and free carbon present in SiC as well as in furnace atmosphere. Amount of SiO_2 present as an oxidation product of SiC at the surface of SiC grains was determined by HF treatment and was found to be 1.6–1.7 wt.%. Values of percent dissolved oxygen in AlN and SiC were taken as supplied by the vendors. Now the most probable reaction in SiO_2 –SiC system¹⁵ under the experimental condition is:



It corresponds to ~2 wt.% loss, when pure SiC was heat treated at the sintering temperature. It was in conformity with the value obtained by the experiment conducted for verification.

In addition to reaction (1), the reaction of SiC with Al_2O_3 (present in AlN) may also contribute to the weight loss as follows:



The reactions (2) and (3) are primarily controlled by alumina in the system. This alumina will come from AlN (present as impurity) which is 0.75 wt.% calculated on the basis of Table 1(b). If reaction (2) is considered, its contribution towards weight loss would be 1.0425 wt.% of AlN, whereas contribution of reaction (1) towards weight loss is 2.133 wt.% of SiC. Therefore, by replacing SiC with AlN, the overall weight loss should be progressively decreased. This explains progressive reduction in weight loss with increasing AlN content. The amount of AlN incorporated is small in comparison with that of SiC. The reaction (3), if considered, was found to contribute insignificantly (0.147 wt.% of AlN) in the weight loss of the samples. On the above basis only the reaction (1) was considered to compare weight loss of the samples (W_O). Both the observed and calculated values are shown in Table 2. The deviation in weight loss, ($W_O - W_C$), (W_O = observed weight loss) against the temperature of sintering is shown in Fig. 8.

Calculated weight loss (W_C) was nearly equal to the observed weight loss (W_O) for the sample containing 5 wt.% AlN fired at 1700 °C and for other samples

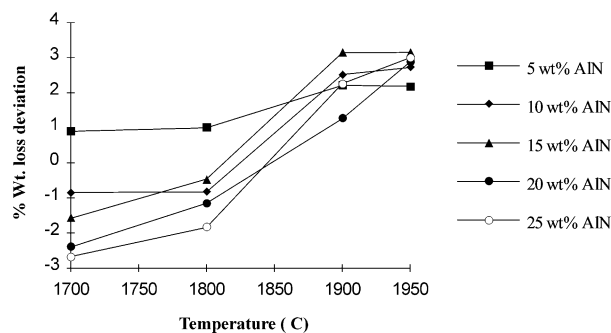


Fig. 8. Plot of wt.% loss deviation ($W_O - W_C$) vs. sintering temperature.

Table 2

Observed and calculated weight loss of the samples sintered at different temperature

Temperature (°C)	Aluminium nitride content (wt.%)									
	5		10		15		20		25	
	C ^a	O ^b	C	O	C	O	C	O	C	O
1700	3.51	3.60	3.38	2.54	3.25	1.67	3.12	0.72	3.00	0.33
1800	3.51	4.51	3.38	2.55	3.25	2.79	3.12	1.97	3.00	1.16
1900	3.51	5.72	3.38	5.90	3.25	6.39	3.12	4.38	3.00	5.26
1950	3.51	5.70	3.38	6.10	3.25	6.40	3.12	6.00	3.00	6.00

^a C = calculated % weight loss.

^b O = observed % weight loss.

$W_O < W_C$ and ($W_C - W_O$) increased with increase in additive content. At 1800 °C, ($W_C - W_O$) was either zero or (+)ve for the samples containing 5–15 wt.% additive. For 20 and 25 wt.% additive $W_O < W_C$. $W_C - W_O < 0$ for all the specimens fired at 1900 °C. ($W_C - W_O$)₁₉₀₀ ≈ ($W_C - W_O$)₁₉₅₀ for all the specimens.

Reaction (1) was substantially suppressed by AlN at lower temperature (<1800 °C) as it was noticed that increasing amount of AlN in the system caused a reduction of weight loss as probably the availability of SiC and so SiO_2 associated with SiC is reduced on account of the reduction in SiC content.

4.2. Structural changes during heat treatment

The change in densification characteristics with sintering temperature could be related to the polymorphic transformation and solid solution formation in SiC–AlN system during gas pressure sintering in N_2 atmosphere.

The XRD-patterns of the SiC–25 wt.% AlN sample fired at 1700 °C revealed a shifting of peak at $d = 2.4840$ Å, relative to that of β -SiC [Fig. 6(a)]. The shifting of peak in relation to that of pure β -SiC was due to the accommodation of AlN in β -SiC. A peak of $2H_{SS}$ was also observed. With increasing the sintering temperature

the relative intensity of the peak corresponding to $2H_{SS}$ increased, indicating more solid solution formation. The main peak for either pure β -SiC ($d=2.517$ Å) or that of AlN (2.70 Å) was absent in all the samples sintered at 1950 °C. The above observation was in conformity to the earlier observations in the similar system. Zangvil et al. [5] proposed that defect-free (or nearly defect-free) β -SiC could not accommodate more than 1–2% AlN, but about 4% AlN could be accommodated into β in 1800–2100 °C to form highly defective β , designated as β' , having a large proportion of hexagonal type sites which was claimed to be responsible for AlN solubility in SiC. Authors also reported that, 25% AlN forms a solid solution with 2H-SiC through a diffusion controlled mechanism.

The unit cell dimension of $2H_{SS}$ was calculated for SiC–25 wt.% AlN sintered at different temperatures and is shown in Fig. 9, where it was evident that the unit cell dimension reduced with the increase in the sintering temperature. Patience et al. [20] asserted that the reduction in unit cell dimension relative to normal 2H-SiC was partly due to the solid solution formation [bond length of Si–N (1.75 Å) < bond length of Si–C (1.88 Å)] and partly due to the formation of Si-vacancies. Thus, the reduction in unit cell dimension with increase in sintering temperature also indicated the increasing solid solution formation.

Therefore, it may be inferred that sintering in the present system was dependent primarily on the conversion of β -SiC to 2H-SiC through an intermediate β' form. So long the cubic SiC was not substantially converted to hexagonal form, sintering remained sluggish. A rapid rise in densification above 1900 °C was thus expected due to the enhanced conversion of 3C-SiC (β) to hexagonal polytypes in the form of $2H_{SS}$.

4.3. Hardness

The increasing amount of solid solution formed was also reflected in the hardness of the sample. The hardness of the sample fired at 1950 °C was also increased with

increasing amount of AlN, a less harder phase than SiC. Apparently the result is contradictory to the reported observations [2]. However, Ruh and Zangvil [21] reported a slight increase in the hardness values of SiC–AlN composites containing less than 35 wt.% AlN i.e. in the high SiC content composites. The continuous increase in hardness value with increase in AlN content up to 25 wt.% AlN in the present system may be explained in the light of solid solution hardening as was observed by Virkar et al. [22], where the hardness of the resultant solid solution formed by AlN and Al_2O_3 showed the same trend [$H_V(AlN)=12.5$ GPa, $H_V(Al_2O_3)=12$ GPa and $H_V(AlN-40 \text{ mol\% } Al_2O_3)=19$ GPa]. Thus, the increase in hardness value of SiC–25 wt.% AlN material sintered at 1950 °C was also an indication of solid solution formation.

A detail microstructural work of the material is under progress and will be reported later.

5. Conclusions

The present work was confined to the SiC–AlN composite in the high-SiC region. SiC–5–25 wt.% AlN could be sintered in N_2 atmosphere under a gas pressure of 6 bar. A nearly pore-free product was obtained for 25 wt.% AlN content at 1950 °C. The nitrogen gas pressure over the sintering system helped to suppress the decomposition of AlN in accordance with Le Chatelier's Principle. Evaporation at the sintering temperature was within the tolerable limit (0.33–6.40%).

Hardness of the sintered samples increased with increasing AlN in the sample. Phase analysis derived from XRD indicated gradual transformation of c-SiC to h-SiC with subsequent formation of solid solution. The increasing hardness with increase in AlN content was explained to be due to the effect of solid solution hardening.

Sintering in this system was primarily diffusion-controlled as the polymorphic transformation of SiC and formation of solid solution was established to be inter-diffusion of two phases, SiC and AlN. Therefore, sintering and related phenomena in the present system were mainly controlled by polymorphic transformation of SiC and solid solution formation between SiC and AlN.

Acknowledgements

The authors are very grateful to Dr. H.S. Maiti, Director, C.G. C.R.I. for his constant encouragement and valuable suggestions during the work and for his kind permission to publish the work. Acknowledgement is also due to the Extra Mural Division, HRD, Council of Scientific and Industrial Research for providing financial assistance.

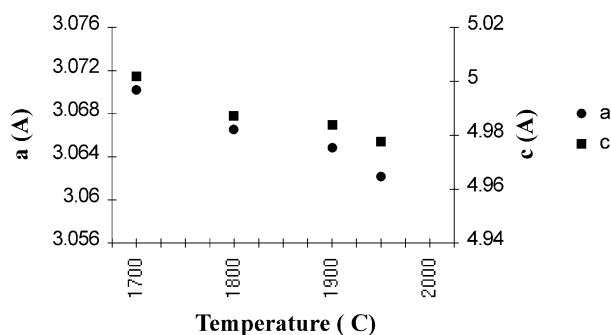


Fig. 9. Plot of unit cell dimension of $2H_{SS}$ for 25 wt.% AlN content vs. sintering temperature.

References

- [1] W. Rafaniello, K. Cho, A.V. Virkar, Fabrication and characteristics of SiC–AlN alloys, *J. Mater. Sci.* 16 (1981) 3479–3488.
- [2] W. Raffeniello, M.R. Plichta, A.V. Virkar, Investigation of phase stability in the system SiC–AlN, *J. Am. Ceram. Soc.* 66 (4) (1983) 272–276.
- [3] Z.C. Jou, S.Y. Kuo, A.V. Virkar, Elevated temperature creep of silicon carbide-aluminium nitride ceramics: Role of grain size, *J. Am. Ceram. Soc.* 69 (11) (1986) C-279–C-281.
- [4] R. Ruh, A. Zangvil, Composition and properties of hot pressed SiC–AlN solid solutions, *J. Am. Ceram. Soc.* 65 (5) (1982) 260–265.
- [5] A. Zangvil, R. Ruh, Phase relationships in the silicon carbide-aluminium nitride system, *J. Am. Ceram. Soc.* 71 (10) (1988) 884–890.
- [6] Z.C. Jou, A.V. Virkar, A.R. Cutler, High temperature creep of SiC densified using a transient liquid phase, *J. Mater. Res.* 6 (9) (1991) 1945–1949.
- [7] W. Cheng, J. Wei, R.R. Lee, Pressureless sintering of AlN–SiC composites, *J. Mater. Sci.* 26 (1991) 2930–2936.
- [8] J. Chen, Q. Tian, A.V. Virkar, Phase separation in the SiC–AlN pseudobinary system: the role of coherency strain energy, *J. Am. Ceram. Soc.* 75 (4) (1992) 809–821.
- [9] Q. Tian, A.V. Virkar, Interdiffusion in SiC–AlN and AlN–Al₂O₃ systems, *J. Am. Ceram. Soc.* 79 (8) (1996) 2168–2174.
- [10] Y.B. Pan, J.H. Qiu, M. Morita, Oxidisation and microhardness of SiC–AlN composite at high temperature, *Mater. Res. Bull.* 33 (1) (1988) 133–139.
- [11] Y.B. Pan, J.H. Qiu, M. Morita, S.H. Tan, D. Jiang, The mechanical properties and microstructure of SiC–AlN particulate composite, *J. Mater. Sci.* 33 (1998) 1233–1237.
- [12] Y. Kuo, A.V. Virkar, Modulated structure in SiC–AlN ceramics, *J. Am. Ceram. Soc.* 70 (6) (1987) C125–C128.
- [13] J.K. Lee, H. Tanaka, H. Rim, Formation of solid solution between SiC–AlN during liquid phase sintering, *Mater. Lett.* 29 (1996) 1–6.
- [14] J.K. Lee, H. Tanaka, S. Otani, Preparation of SiC–AlN composites by liquid phase sintering and microstructure, *J. Ceram. Soc. Japan* 103 (9) (1995) 873–877.
- [15] T. Grande, H. Sommerset, E. Hagen, K. Wiik, Mari-Ann Einarsrud, Effect of weight loss on liquid phase sintered silicon carbide, *J. Am. Ceram. Soc.* 80 (4) (1997) 1047–1052.
- [16] T.I. Mah, K.A. Keller, S. Samsbasivan, R.J. Kerans, High-temperature environmental stability of the compounds in the Al₂O₃–Y₂O₃ system, *J. Am. Ceram. Soc.* 80 (4) (1997) 874–878.
- [17] W. Rafaniello, K. Cho, A.V. Virkar, Fabrication and characterisation of SiC–AlN alloys, *J. Mater. Sci.* 16 (1985) 3479–3488.
- [18] M.M. Patience, P.J. England, D.P. Thompson, K.H. Jack, Ceramic alloys of silicon carbide with aluminium nitride and nitrogen, ceramic components for engines, in: S. Somiya, E. Kanai, K. Anto (Eds.), *Proceedings of the first international symposium, 1983, Japan*, Elsevier Applied Science, London and New York, 1983, pp. 473–479.
- [19] L.D. Bentsen, D.P.H. Hasselman, Effect of hot-pressing temperature on the thermal diffusivity/conductivity of SiC–AlN composites, *J. Am. Ceram. Soc.* 66 (3) (1983) C40–41.
- [20] R. Ruh, A. Zangvil, J. Barlowe, Elastic properties of SiC, AlN and their solid solutions and particulate composites, *Am. Ceram. Soc. Bull.* 64 (10) (1985) 1368–1373.
- [21] R. Ruh, A. Zangvil, Composition and properties of hot pressed SiC–AlN solid solutions, *J. Am. Ceram. Soc.* 65 (5) (1982) 260–265.
- [22] S.-Y. Kuo, A.V. Virkar, Phase equilibria and phase transformation in the aluminium nitride-aluminium oxycarbide pseudobinary system, *J. Am. Ceram. Soc.* 72 (40) (1989) 540–550.